INTERNATIONAL JOURNAL OF HYDROGEN ENERGY 45 (2020) 30783–30791

Available online at www.sciencedirect.com

ScienceDirect

journal homepage: www.elsevier.com/locate/he

Structural evolution, mechanical, electronic and vibrational properties of high capacity hydrogen storage TiH_4

Selgin Al [a,*], Cihan Kurkcu [b], Cagatay Yamcicier [c]

[a] Department of Environmental Protection Technologies, Izmir Democracy University, 35140, Izmir, Turkey
[b] Department of Electronics and Automation, Kirsehir Ahi Evran University, Kırşehir, Turkey
[c] Institute of Science, Gazi University, Ankara, Turkey

GRAPHICAL ABSTRACT

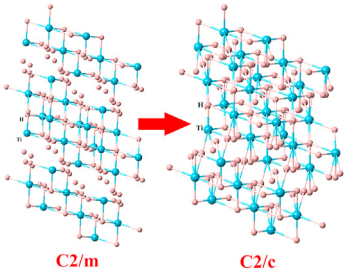

ARTICLE INFO

Article history:
Received 11 May 2020
Received in revised form
6 July 2020
Accepted 13 August 2020
Available online 1 September 2020

Keywords:
Molecular dynamic simulation
High pressure
Hydrogen storage
Stability

ABSTRACT

Titanium tetra hydride is considered for hydrogen storage purposes. Firstly, formation energy, hydrogen desorption temperature and gravimetric hydrogen density of TiH_4 is computed. Secondly, an ab initio constant pressure molecular dynamic simulation under pressure is performed to reveal behaviour of TiH_4 for the first time. The result exhibits two phase transitions successively. C2/m phase of TiH_4 transforms into C2/c phase at 40 GPa simulation pressure. Then, elastic constants of phases are determined to examine mechanical stability of phases. Based on the evolution of elastic constants, it is found that C2/m phase fulfils Born stability criteria for a monoclinic structure, indicating that C2/m phase is mechanically stable whereas C2/c phase is not mechanically stable. Additionally, several critical parameters which are important for hydrogen storage such as brittleness and ductility, Young and Shear modulus are obtained and analysed. In addition, electronic structures of phases are calculated and evaluated. Finally, dynamic stability from phonon dispersion curves is examined. C2/m phase is also found to be dynamically stable.

* *Corresponding author.*
E-mail address: selgin.al@idu.edu.tr (S. Al).
https://doi.org/10.1016/j.ijhydene.2020.08.108

Introduction

Utilization of renewable energy is a necessity for reducing the impacts of global warming and greenhouse gases. This requires development of sustainable energy processes and materials. Electricity from hydrogen is one of the most promising way of accomplishing this purpose. In order to drive wide spread use of hydrogen energy, a few obstacles have to be overcome such as storage. There are several alloys and compounds have been under investigation to find better materials with high hydrogenation/dehydrogenation rates, low decomposition temperature and high capacity.

Metal hydrides have been investigated as high capacity hydrogen storage materials intensively lately [1]. Vanadium, zirconium, titanium and uranium are the most common metals that are considered for hydrogen storage. Especially, vanadium based hydrides are investigated due to their high hydrogen solubility, however there are still issues to be overcome with these hydrides since they suffer from pulverisation and reversibility [2–4]. Magnesium dehydrides also have been studied extensively owing to their low cost, light weight and high capacity [5,6]. Titanium is known to be reactive with hydrogen to form metal hydride. It is used as electrodes in batteries, catalysts and also in hydrogen storage. Mechanical properties of titanium hydride was investigated by Setoyama et al. [7]. Their study demonstrated that titanium hydride has smaller elastic moduli than titanium, they also suggested that hydrogen uptake causes a decrease in mechanical strength of titanium, thus titanium hydrides may become brittle. However, there is no adequate characteristics information and analysis to draw this conclusion for all mechanical strength of titanium hydrides. Thermodynamic properties of titanium hydrides were computed using ab initio calculations by Olsson et al. [8]. Also, high capacity metal tetra hydrides were proposed by Pan [9]. Pan theoretically investigated 21 metal tetrahydrides including VH_4 and TiH_4 using ab initio calculations. However, their calculations do not have detailed characterisations such as elastic constants to evaluate mechanical stability. Also, ground state stabilities and properties are not investigated. A structural search under high pressure for various hydrides including titanium was carried out by Zhao et al. [10] and novel stable phases of $R\bar{3}$ -TiH_3, $P4_2/mnm$-TiH_3 and Ibam-$TiH_{2.5}$ were reported in this research. Recently, titanium-hydrogen interaction at high pressure and temperature has been studied using molecular dynamic calculations [11]. The result indicated that diffusion law can be applied for dissolution of titanium in dense hydrogen at mega bar pressure and T > 3000 K. An ab initio calculation has been carried out for a cubic CaF_2-type structure ($Fm\bar{3}m$ space group) TiH_2 and reported mechanical instability due to negative C_{44} value [12]. On the other hand, in an another study carried out by Liu et al. [13] a mechanical stability at zero pressure and temperature based on the evaluation of lattice constants was reported for tetragonal-TiH_2. In a very recent study, elastic and thermodynamic properties of tetragonal TiH_2 (P42/mnm) and orthorhombic TiH_2 (Pnma) were predicted using first principle calculations [14]. There are also other studies that focus on titanium hydrides stability and properties [15,16] for hydrogen storage. It is clear that titanium hydrides have been considered much extensive than titanium tetra hydrides for hydrogen storage purposes. Nevertheless, TiH_2 is reported to be extremely brittle in studies [17,18]. The transportable capacity is a critical parameter for hydrogen storage materials, thus TiH_2 is not ideal as a storage material. However, it is reported that TiH_2 can catalyse and improve hydrogenation and dehydrogenation processes and can be used as catalysts [19,20]. TiH_2 and titanium-based intermetallics have been considered for improving the kinetics of magnesium hydrogenation [21]. The impact of TiH_2 and TiO_2 on desorption properties of MgH_2 was investigated experimentally by Daryani et al. [22]. Their results also suggest that dehydrogenation temperature of MgH_2 decreased as a result of kinetic improvements of dehydrogenation process.

These attempts to find superior hydrogen storage materials using computational methods can provide three critical advantages to the research world; understanding atomic scale properties of materials, estimate results and potential materials, reveal all properties of materials such as structural, electronic, thermodynamic and stabilities prior to experiments [23]. First principle calculation is one of the tools that can give substantial information about these properties in a great detail. For example, by calculating the total energy or energy difference

Table 1 – Atomic positions for C2/m and C2/c phases of TiH_4.

Phases	Atom	Atomic positions		
		x	y	z
C2/m (#12)	Ti	0.845600	0.000000	0.645237
	H	0.145800	0.000000	0.558300
	H	0.451650	0.000000	0.267512
	H	0.081387	0.000000	0.129300
	H	0.216800	0.000000	0.127300
C2/c (#15)	Ti	0.869138	0.285050	0.843731
	H	0.151600	0.284438	0.782888
	H	0.914550	0.214188	0.097531
	H	0.107306	0.849019	0.032934
	H	0.143681	0.493019	0.036478

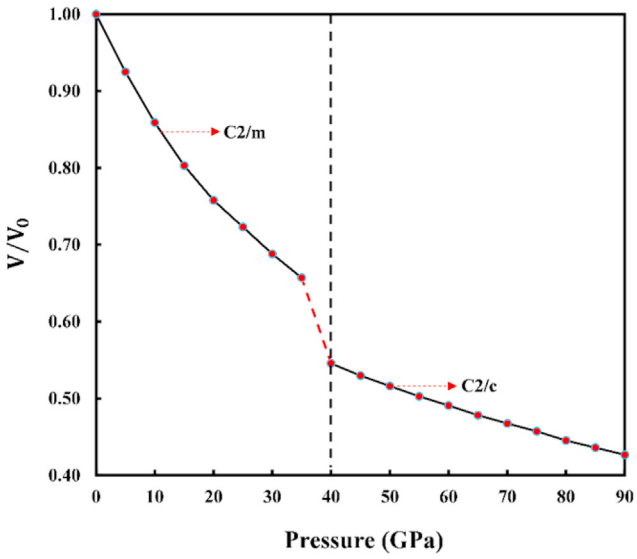

Fig. 1 – Volume change of TiH_4 under hydrostatic pressure (simulation pressure).

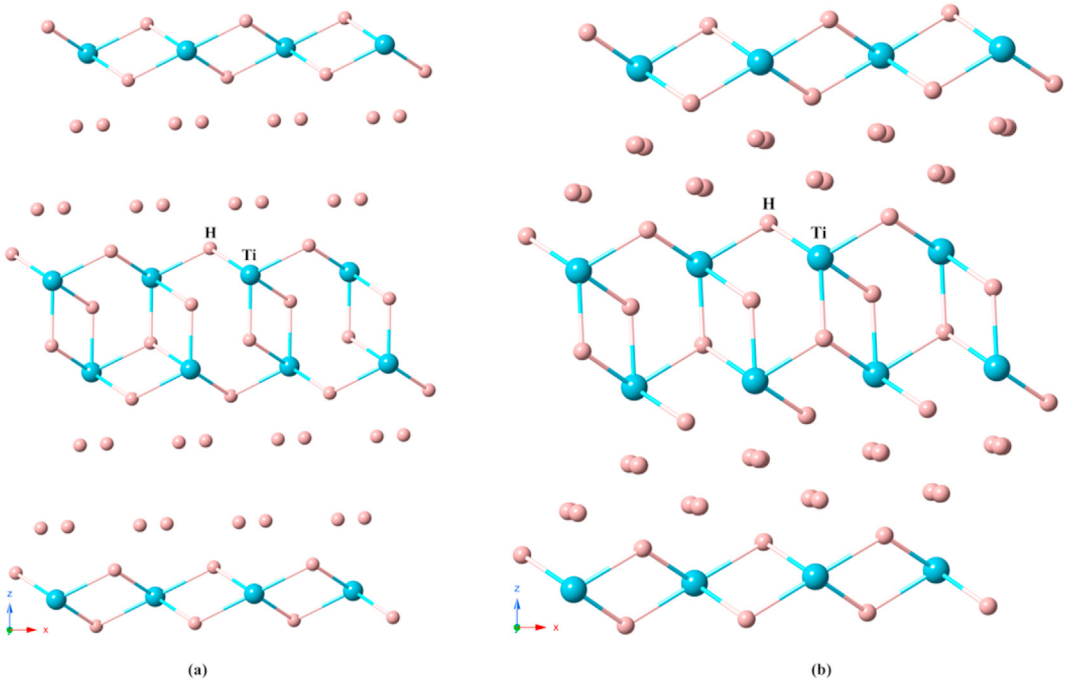

Fig. 2 – Structural evolution of TiH_4: C2/m at 0 GPa (a) and C2/c at 40 GPa (b).

between a perfect crystal and a distorted crystal can allow one to predict thermodynamic properties. Moreover, by removing atoms and determining the force in the remaining atoms can be used to obtain phonon modes and thus, vibrational properties of the material. The motivation of this work lies in finding the most stable phases of high hydrogen capacity TiH_4 under pressure and revealing physical properties of each phase using first principle calculations. The study starts with calculating formation enthalpy, gravimetric hydrogen density (GHD) and hydrogen desorption temperature of TiH_4 and continues with structural evolution under pressure. The mechanical strength of each stable phases along with electronic and vibrational properties have also been predicted and analysed.

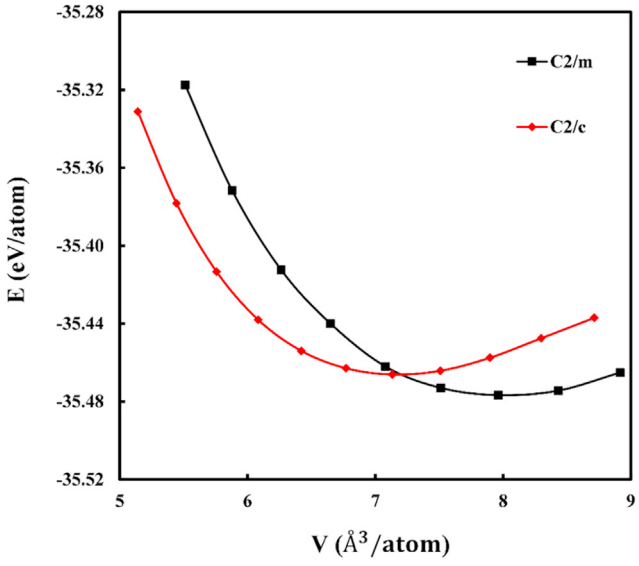

Fig. 3 – Energy-volume relations of C2/m and C2/c phases.

Method

The ab initio computations were adopted within the density functional theory as implemented in SIESTA method in order to calculate structural, elastic, electronic and vibrational properties of TiH_4 [24]. Perdew-Burke-Ernzerhof, generalised gradient approximation (PBE-GGA) was used for the exchange correlation potential [25]. Troullier-Martins type norm-conserving pseudo-potential for Ti and H atoms were adopted [26]. Double-zeta (DZ) basis sets of localized atomic orbitals were taken into account for all computations. As a result of optimisation, 350 Rydberg (Ry) mesh cut-off energy was utilised to compute the Hartree, exchange, and correlation contribution to the total energy and Hamiltonian. TiH_4 was modelled using 2x2x2 cells with periodic boundary conditions for 160 atoms supercells. The Brillouin zones (BZ) were sampled with the 4x8x2 and 6x12x2 Monkhorst-Pack k-point mesh for C2/m and C2/c structures, respectively [27]. These k-point values were obtained from independent tests. In general, a particular k-point grid then repeats with a finer k-point grid (i.e. more k-points) was considered. Finer k-point grids were tried until all converged to the wanted accuracy. Structural optimizations were carried out via the conjugate gradient [28] until the residual force acting on all atoms was lower than 0.01 eV/Å and pressure was gently risen by steps of 5 GPa via this method to the system. To evaluate every minimization step, the KPLOT program and the RGS algorithm was adopted that provide detailed information about the space groups, atomic positions and lattice parameters of an analysed structure [29,30]. For the energy–volume calculations, we used the unit cells of the C2/

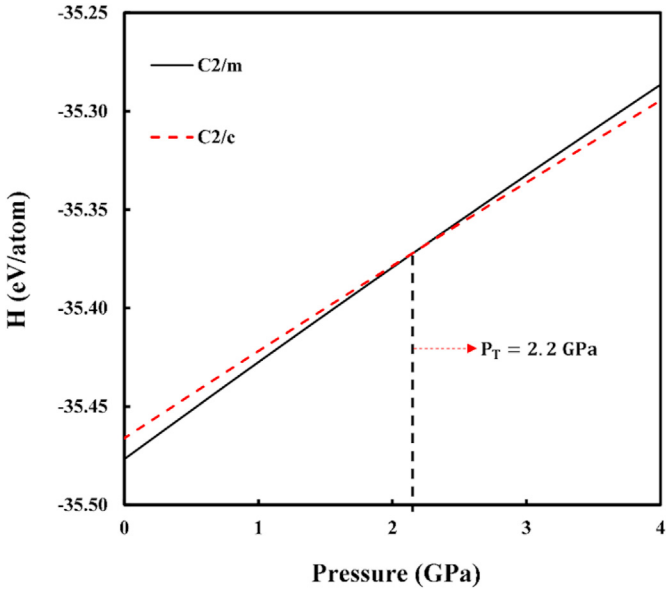

Fig. 4 – Enthalpy changes of C2/m and C2/c phases versus pressure.

m and C2/c structures. Enthalpy calculation was also made using these energy-volume data.

Results and discussion

Hydrogen storage properties and structural evolution

Prior to investigate mechanical properties of TiH_4, the equilibrium phase of TiH_4 is determined at zero pressure and temperature as monoclinic with the space group C/2 m. Table 1 displays atomic positions of phases of TiH_4. Subsequently, formation enthalpy of C/2 m phase of TiH_4, gravimetric hydrogen density and hydrogen desorption temperature are computed. Formation enthalpy of C/2 m phase of TiH_4 is obtained as −0.650 eV/atom, specifics are given in Ref. [31].

Gravimetric hydrogen density is a key parameter to determine to search for superior hydrogen storage material before proceeding further studies such as atomic structure estimation and mechanical stability. The gravimetric hydrogen density of TiH_4 is estimated by using the equation below [32,33];

$$C_{wt\%} = \left(\frac{(H/M)M_H}{M_{Host} + (H/M)M_H} \times 100 \right)\% \quad (1)$$

where H/M is hydrogen to metal ratio, M_H is molar mass of hydrogen and M_{Host} is molar weight of host material. The obtained GDH of TiH_4 is about 7.77 wt %. This may help to achieve the recently set value (5.5 wt %) by US DOE for solid state hydrogen storage for a complete system [34].

In addition to GHD of TiH_4, hydrogen desorption temperature is predicted to evaluate the applicability of TiH_4 as a storage material. Hydrogen desorption temperature is a crucial parameter since it determines the temperature that is necessary for release of hydrogen from host material. The standard Gibbs energy $\Delta G = \Delta H - T\Delta S$ where ΔH and ΔS are the enthalpy and entropy changes of the dehydrogenation reaction, respectively can be used to predict hydrogen desorption temperature computationally [31,35]. Gibbs energy goes to zero at the decomposition temperature and under a constant pressure. Therefore, hydrogen desorption temperature can be predicted by $\Delta H = T\Delta S$. The hydrogen entropy change is previously determined as 130.7 J/mol. K [36,37]. The following equation is then adopted to carry out this calculation;

$$\Delta H = T_d \times \Delta S \quad (2)$$

where hydrogen desorption temperature is represented by T_d. Hydrogen desorption temperature is predicted as 480.87 K. This temperature range may be considered close to the target set by US DOE which is 85 °C for on-board applications [38], however, could be much useful for stationary applications.

The variation in volume of TiH_4 is obtained by applying first principles molecular dynamic simulation to determine structural evolution under pressure thermodynamically and presented in Fig. 1. The volume calculations in Fig. 1 have been carried out by using a simulation cell including 160 atoms with a 2 × 2 × 2 cells and periodic boundary conditions. V/V_o implies a reduction in volume which is also a ratio of volume at any pressure to volume at zero pressure. The simulation cell volume decreases sharply and at a pressure of 35 GPa a dramatic volume collapse is seen. At a 40 GPa pressure, a phase transition from C2/m phase to C2/c phase is observed. This severe volume change indicates a first-order phase transition in TiH_4.

The structural evolution of TiH_4 is also predicted and shown in Fig. 2. The structural change of C/2 m phase of TiH_4 tetra hydride is studied in this work for the first time as far as the authors' knowledge. As can be seen from Fig. 2 that the C2/m phase of TiH_4 transforms into C2/c phase at 40 GPa simulation pressure. The atomic positions of atoms of this phase is also given in Table 1.

The constant pressure simulations can lead to estimation of higher transitions pressures compared to actual experimental transition pressures and can indicate high activation

Table 2 – Elastic constants (GPa) of TiH_4 phases.

Phases	C_{11}	C_{12}	C_{13}	C_{15}	C_{22}	C_{23}	C_{25}	C_{33}	C_{35}	C_{44}	C_{46}	C_{55}	C_{66}
C2/m	139.280	53.797	2.946	0.953	127.113	3.611	1.159	11.608	0.001	3.235	1.078	0.505	18.502
C2/c	348.257	127.414	120.133	0.00	355.540	59.414	0.000	175.792	0.000	3.109	0.000	−144.781	114.267

barrier to transform from one phase to another [39–43]. This higher estimation is well recognised and expected due to application of pressure to a solid in a very short time scale, consideration of perfect boundary conditions for the simulation cell and ignorance of defects and surface effect etc. Due to the listed restrictions above, thermodynamic theorem is commonly used to compute actual transition pressures since it does not take into account parameters such as activation barrier and restrictions. Therefore, the energy-volume calculations are performed to obtain transitions pressures for C2/m to C2/c phases.

The thermodynamic principle of Gibbs free energy (G) is adopted to evaluate structural transformation of phases which is given by;

$$G = E_{tot} + PV - TS \tag{3}$$

where E is the total energy, P is the pressure, V is the volume and S is the entropy.

$$\begin{aligned} &C_{33}C_{55} - C_{32}^2 > 0, \qquad C_{44}C_{66} - C_{46}^2 > 0, \\ &C_{22} + C_{33} - 2C_{23} > 0 \qquad C_{11} + C_{22} + C_{33} + 2(C_{12} + C_{13} + C_{23}) > 0 \\ &C_{22}(C_{33}C_{55} - C_{35}^2) + 2C_{23}C_{25}C_{35} - C_{23}^2C_{55} - C_{25}^2C_{33} > 0, \\ &2\left[C_{15}C_{25}(C_{33}C_{12} - C_{13}C_{23}) + C_{15}C_{35}(C_{22}C_{13} - C_{12}C_{23}) + C_{25}C_{35}(C_{11}C_{23} - C_{12}C_{13})\right] - \left[C_{15}^2(C_{22}C_{33} - C_{23}^2) + C_{25}^2(C_{11}C_{33} - C_{13}^2) + \right. \\ &\left. C_{35}^2(C_{11}C_{22}\upsilon C_{12}^2)\right] + gC_{55} > 0, \\ &with \;\; g = C_{11}C_{22}C_{33} - C_{11}C_{23}^2 - C_{22}C_{13}^2 - C_{33}C_{12}^2 + 2C_{12}C_{13}C_{23} \end{aligned} \tag{6}$$

At zero temperature, this equation becomes equal to enthalpy as;

$$H = E_{tot} + PV \tag{4}$$

In order to compute enthalpy of both phases, energies of phases for different volumes are predicted by scaling the lattice parameters and atomic positions uniformly and the result is presented in Fig. 3. Then the obtained data is fitted to the third-order Birch-Murnaghan equation of state [44,45] given below;

$$P = 1.5B_0\left[\left(\frac{V}{V_0}\right)^{-\frac{7}{3}} - \left(\frac{V}{V_0}\right)^{-\frac{5}{3}}\right] x \left\{1 + 0.75\left(B_0^{apos;} - 4\right)\left[\left(\frac{V}{V_0}\right)^{-\frac{2}{3}} - 1\right] \times \right\} \tag{5}$$

where pressured is given by P, volume at the pressure is given by V, V_0, B_0 and $B_0^{'}$ are the volume, bulk modulus and its pressure derivate at 0 GPa, respectively.

From this curve P can be obtained as $P = dE_{tot}/dV$ and finally the enthalpy values of phases. It is expected that the most stable phase will have the lowest enthalpy at zero temperature and at a known pressure. Since both phases will have the same enthalpy values when a structural transformation occurs, the transition pressure can be easily estimated by equating both enthalpy values of phases. The predicted enthalpy values of phases are exhibited in Fig. 4. As Fig. 4 indicates that the phases cross each other at 2.22 GPa, suggesting that the phase transition from C2/m to C2/c phase occurs at 2.2 GPa.

Elastic properties and mechanical stability

Elastic properties of phases are also computed in order to gather information about atomic bonding, phonon properties, stiffness, ductility, brittleness and mechanical stabilities. There are thirteen independent elastic constants are defined for a low symmetry monoclinic structure as C_{ij} [46,47]. For a monoclinic structure, famous Born stability criteria for an unstressed single crystal for mechanical stability is defined as [48,49];

Mechanical properties must be revealed for hydrogen storage materials to be transported. These properties are examined by elastic constants and also their derivation can provide other parameters such as Shear modulus, Young modulus and Poisson's ratio [50]. The thirteen independent elastic constants of C2/m and C2/c phases are summarised in Table 2. First of all, it can be realised that the computed elastic constants of C2/m phase meet Born stability criteria given in Eq. (6) whereas C2/c phase does not meet the criteria due to having a negative value of C_{55}. Thus, it can be concluded that C2/m phase is mechanically stable, on the other hand, C2/c phase is not mechanically stable. Unfortunately, there is no data exist for comparison in literature for these phases of TiH_4

Table 3 – The calculated Bulk modulus (*B*), Shear modulus *G* (GPa), *G/B and B/G* ratios, Poisson's ratios (*σ*) *and* Young's modulus *E* (GPa) of phases of TiH_4.

Phases	B	G	G/B	B/G	σ	E
C2/m	27.595	10.459	0.379	2.638	0.332	27.857
C2/c	153.363	31.428	0.204	4.880	0.404	88.254

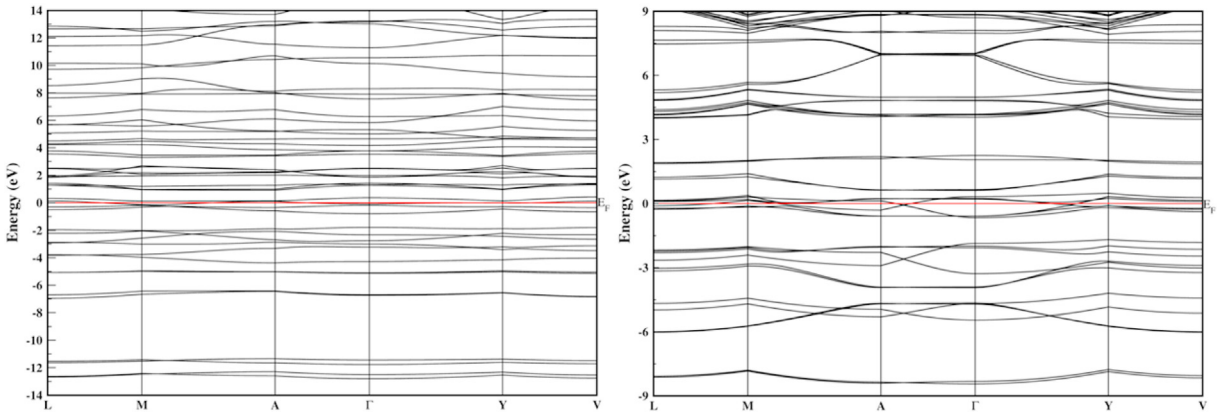

Fig. 5 – The calculated electronic band structures of TiH_4 at 0 GPa and at 40 GPa.

tetra hydride. Therefore, this study can serve as a reference for future titanium tetra hydrides studies as a hydrogen storage material and also other applications.

By using the data in Table 2, bulk modulus of phases are obtained. Bulk modulus is a degree of resistivity towards volume change which is executed by an applied pressure. This can provide substantial information about average bound strength because of having a strong correlation with cohesive and binding energies of material's atoms [51,52]. Higher bulk modulus means higher resistivity against volume change [53]. These driven results are provided in Table 3. By examining bulk modulus of phases from Table 3, it can be said that C2/c has higher ability to show resistance against volume change than C2/m phase. For the sake of the argument, the results of C2/m monoclinic phase of TiH_4 may be compared with tetragonal (I4mmm) and orthorhombic (Pnma) phase of TiH_2 [14] as well. Pan et al. reported bulk modulus of tetragonal TiH_2 as 136.7 and 139.5 for orthorhombic TiH_2. By comparing those results, it can be predicted that orthorhombic TiH_2 can resist volume change more than tetragonal TiH_2 and monoclinic TiH_4 with monoclinic TiH_4 being the least resistive solid.

Shear modulus (G) of a solid defines its ability to resist a shape change and higher Shear modulus is an indication of hardness. Shear modulus of C2/m phase of TiH_4 is found to be 10.4 in our study whereas 32.6 and 51.5 Shear modulus were reported for tetragonal and orthorhombic TiH_2 by Pan et al. [14]. This suggests that titanium dihydrides show stronger deformation resistance compared to titanium tetra hydride.

Brittleness-ductility of hydrogen storage materials are critical for on-board application. Thus, B/G ratio of TiH_4 is also determined. This well-known ratio is defined by Pugh [54] and set as 1.75. In the case of higher value, the material is classified as ductile material, otherwise it is classified as brittle material. As Table 3 displays that TiH_4 has higher B/G ratio than 1.75. That classifies this material as a ductile material which is a good property for practical hydrogen storage applications.

Poisson's ratio imparts material's chemical bonding nature and stability against shear. Larger ratio means good plasticity [55]. Moreover, it is reported that the value is around 0.1 for covalent bonding and around 0.25 or higher for ionic bonding [56,57]. Based on that, our results suggest that ionic bonding is dominant in TiH4.

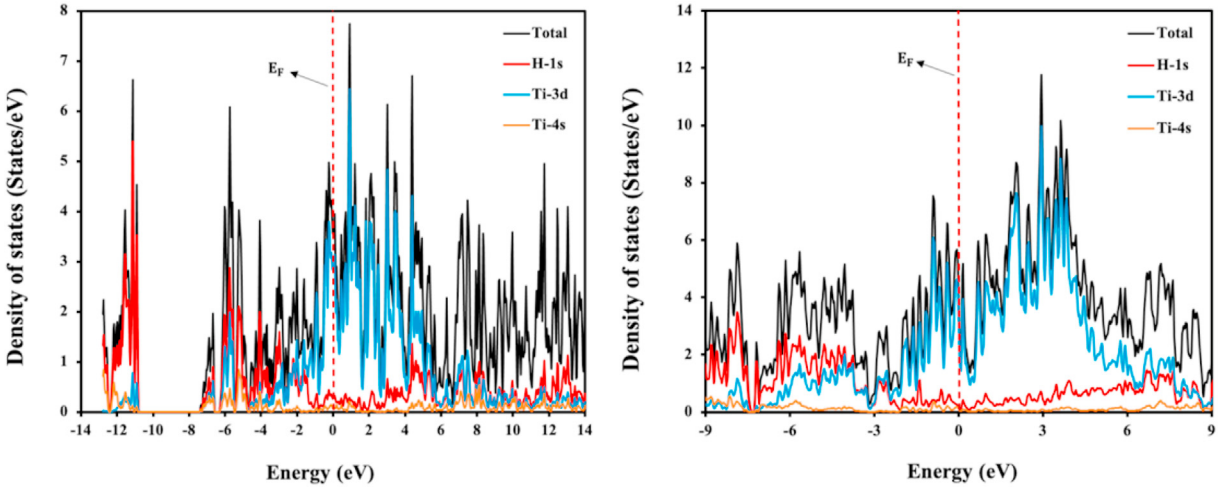

Fig. 6 – The partial and total DOS of TiH_4 at 0 GPa and at 40 GPa.

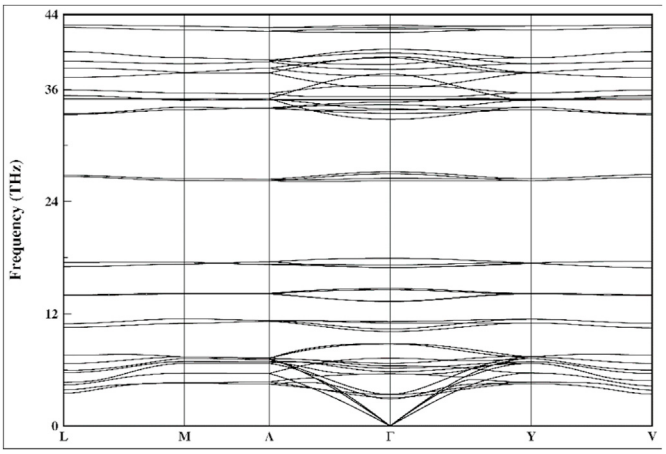

Fig. 7 – The phonon dispersion curves of TiH_4 at 0 GPa.

Young Modulus (*E*) of a material is defined as the ratio of tensile stress to tensile strain. Larger Young modulus means better stiffness. It is also defined as resistance against changes in the x-direction under applied pressure. Based on the data given in Table 3, it can be predicted that C2/c phase of TiH_4 shows better stiffness than C2/m phase of TiH_4 and the stiffness of material increases with applied pressure.

Electronic density of states and phonon properties

In addition to mechanical stability evaluation, the electronic band structures of TiH_4 phases are calculated along with the high symmetry directions and the results are presented in Figs. 5 and 6. Fermi energy level is set to 0 eV in both figures. As Fig. 5 displays that there is no band gap exist at both pressures. Also, valence and conduction bands seem to cross each other, suggesting that TiH_4 is a conducting material in both phases and show metallic behaviour.

The partial and total density of states (DOS) of phases is also computed and shown in Fig. 6. The contribution to conductivity seems to be mainly because of Ti-3d orbitals in the conduction band with a little contribution from H-1s orbitals for both phases. It is seen that there is no dramatic change in the electronic states due to phase transformation.

Lastly, the phonon dispersion curves of TiH_4 for C2/m phase at 0 GPa is calculated and given in Fig. 7. The phonon dispersion curve of C2/c phase is not computed since this phase is mechanically unstable, it is expected that it will also be dynamically unstable. The phonon curve for C2/m phase shows no imaginary frequency, indicating that C2/m phase is dynamically stable.

Conclusion

Ab initio calculations have been applied to study hydrogen storage properties, structural evolution, elastic, electronic and vibrational properties of titanium tetra hydride. The GHD of TiH_4 is found to be 7.77 wt % along with 480.87 K hydrogen desorption temperature. These values may help to achieve recently revised US DOE target as 5.5 wt % for a complete system [34] for practical applications. High pressure simulations show C2/m and C2/c monoclinic phases for TiH_4. C2/m phase at 0 GPa is found to be mechanically stable whereas C2/c phase exhibits mechanical instability. Several critical parameters have been obtained. B/G ratios of phases indicate that both phases have ductile nature which is a wanted property for on-board hydrogen storage applications. Additionally, electronic band structures and partial and total density of states for two phases are obtained. The results reveal that both phases demonstrate metallic behaviour. Finally, the phonon dispersion curve is obtained for C2/m phase and no imaginary frequency is found. This implies that C2/m phase is also dynamically stable. Sadly, the authors cannot find any available data in literature to compare for these values for titanium tetra hydride. However, this work can serve as a basis for future research and applications.

Declaration of competing interest

The authors declare that they have no known competing financial interests or personal relationships that could have appeared to influence the work reported in this paper

REFERENCES

[1] Sakintuna B, Lamari-Darkrim F, Hirscher M. Metal hydride materials for solid hydrogen storage: a review. Int J Hydrogen Energy 2007;32(9):1121–40.
[2] Kumar S, et al. Development of vanadium based hydrogen storage material: a review. Renew Sustain Energy Rev 2017;72:791–800.
[3] Kumar S, et al. Cyclic hydrogen storage properties of VTiCrAl alloy. Int J Hydrogen Energy 2018;43(14):7096–101.
[4] Liu Z, et al. Effects of alloying elements (Al, Mn, Ru) on desorption plateau pressures of vanadium hydrides: an experimental and first-principles study. Int J Hydrogen Energy 2018;43(46):21441–50.
[5] Lefevre G, et al. Hydrogen storage in MgX (X = Cu and Ni) systems - is there still news? J Power Sources 2018;402:394–401.

[6] Paskaš Mamula B, et al. Electronic structure and charge distribution topology of MgH_2 doped with 3d transition metals. Int J Hydrogen Energy 2014;39(11):5874–87.
[7] Setoyama D, et al. Mechanical properties of titanium hydride. J Alloys Compd 2004;381(1):215–20.
[8] Olsson PAT, et al. Ab initio thermodynamics investigation of titanium hydrides. Comput Mater Sci 2015;97:263–75.
[9] Pan Y. Theoretical discovery of high capacity hydrogen storage metal tetrahydrides. Int J Hydrogen Energy 2019;44(33):18153–8.
[10] Zhao XY, et al. Theoretical study of M-H (M=Ti, V, Zr or Nb) structure phase diagram at high pressures. Int J Hydrogen Energy 2019;44(26):13592–605.
[11] Mazitov AB, Oganov AR, Yanilkin AV. Titanium-hydrogen interaction at megabar pressure. arXiv preprint arXiv:1802.08292 2018.
[12] Chihi T, Fatmi M, Bouhemadou A. Structural, mechanical and electronic properties of transition metal hydrides MH_2 (M = Ti, Zr, Hf, Sc, Y, La, V and Cr). Solid State Sci 2012;14(5):583–6.
[13] Liu X, Tang B, Zhang Y. Ab initio calculations of structure and thermodynamic properties of tetragonal-TiH_2 under high temperatures and pressures. Eur Phys J Appl Phys 2013;64(1).
[14] Pan Y, Chen S. Exploring the novel structure, transportable capacity and thermodynamic properties of TiH_2 hydrogen storage material. Int J Energy Res 2020;44(6):4997–5007.
[15] Barthelemy H, Weber M, Barbier F. Hydrogen storage: recent improvements and industrial perspectives. Int J Hydrogen Energy 2017;42(11):7254–62.
[16] Manivasagam TG, et al. Synthesis and electrochemical properties of binary MgTi and ternary MgTiX (X = Ni, Si) hydrogen storage alloys. Int J Hydrogen Energy 2017;42(37):23404–15.
[17] Gao GY, et al. *Pressure induced phase transitions in TiH_2*. J Appl Phys 2013;113(10):4.
[18] Bhosle V, et al. *Dehydrogenation of TiH_2*. Mater Sci Eng 2003;356(1):190–9.
[19] Íñiguez J, et al. Structure and hydrogen dynamics of pure and Ti-doped sodium alanate 2004;70(6):060101.
[20] Yildirim T, Ciraci SJPrl. Titanium-decorated carbon nanotubes as a potential high-capacity hydrogen storage medium 2005;94(17):175501.
[21] Rizo-Acosta P, Cuevas F, Latroche M. Optimization of TiH_2 content for fast and efficient hydrogen cycling of MgH_2-TiH_2 nanocomposites. Int J Hydrogen Energy 2018;43(34):16774–81.
[22] Daryani M, et al. Effects of Ti-based catalysts on hydrogen desorption kinetics of nanostructured magnesium hydride. Int J Hydrogen Energy 2014;39(36):21007–14.
[23] Wimmer E. The growing importance of computations in materials science. Current capabilities and perspectives. Materials Science-Poland 2005;23(2):325–45.
[24] Ordejón P, Artacho E, Soler JM. Self-consistent order-N density-functional calculations for very large systems. Phys Rev B 1996;53(16):R10441.
[25] Perdew JP, Burke K, Ernzerhof M. Generalized gradient approximation made simple. Phys Rev Lett 1996;77(18):3865–8.
[26] Troullier N, Martins JL. Efficient pseudopotentials for plane-wave calculations. Phys Rev B 1991;43(3):1993–2006.
[27] Monkhorst HJ, Pack JD. Special points for Brillouin-zone integrations. Phys Rev B 1976;13(12):5188–92.
[28] Ceperley DM, Alder BJ. Ground state of the electron gas by a stochastic method. Phys Rev Lett 1980;45(7):566.
[29] Hundt R, et al. Determination of symmetries and idealized cell parameters for simulated structures. J Appl Crystallogr 1999;32(3):413–6.
[30] Hannemann A, et al. A new algorithm for space-group determination. J Appl Crystallogr 1998;31(6):922–8.
[31] Bhihi M, et al. Hydrogen storage of $Mg_{1-x}M_xH_2$ (M = Ti, V, Fe) studied using first-principles calculations. Chin Phys B 2012;21(9):097501.
[32] Broom DP. Hydrogen storage materials; the characterisation of their storage properties. 1 ed. Springer-Verlag London; 2011.
[33] Al S. Investigations of physical Properties of $XTiH_3$ and Implications for solid state hydrogen storage. Z Naturforsch 2019:1023.
[34] Tian M, et al. Nanoporous polymer-based composites for enhanced hydrogen storage 2019;25(4):889–901.
[35] Zhang J, et al. Strain effect on structural and dehydrogenation properties of MgH_2 hydride from first-principles calculations. Int J Hydrogen Energy 2013;38(9):3661–9.
[36] Zeng Q, et al. Evaluation of the thermodynamic Data of CH_3SiCl_3 Based on quantum chemistry calculations. J Phys Chem Ref Data 2006;35(3):1385–90.
[37] Al S, Kurkcu C, Yamcicier C. High pressure phase transitions and physical properties of Li_2MgH_4; implications for hydrogen storage. Int J Hydrogen Energy 2020;45(7):4720–30.
[38] Aslan MY, Uner D. Fundamentals of hydrogen storage processes over Ru/SiO_2 and Ru/Vulcan. Int J Hydrogen Energy 2019;44(34):18903–14.
[39] Yamcicier C, Merdan Z, Kurkcu C. Investigation of the structural and electronic properties of CdS under high pressure: an ab initio study. Can J Phys 2017;96(2):216–24.
[40] Kürkçü C, et al. Investigation of structural and electronic properties of β-HgS: molecular dynamics simulations. Chin J Phys 2018;56(3):783–92.
[41] Durandurdu M. Orthorhombic intermediate phases for the wurtzite-to-rocksalt phase transformation of CdSe: an ab initio constant pressure study. Chem Phys 2010;369(2–3):55–8.
[42] Kürkçü C, Merdan Z, Öztürk H. Theoretical calculations of high-pressure phases of NiF_2: An ab initio constant-pressure study. Russ J Phys Chem 2016;90(13):2550–5.
[43] Kürkçü C, Merdan Z, Öztürk H. Pressure-induced phase transitions and structural properties of CoF2: an ab-initio molecular dynamics study. Solid State Commun 2016;231:17–25.
[44] Birch F. Finite elastic strain of cubic crystals. Phys Rev 1947;71(11):809.
[45] Murnaghan F. The compressibility of media under extreme pressures. Proc Natl Acad Sci USA 1944;30(9):244.
[46] Liu Q-J, Liu F-S, Liu Z-T. Structural, mechanical, and electronic properties of monoclinic N 2 H 5 N 3 under pressure. Braz J Phys 2015;45(4):399–403.
[47] Edrees SJ, Shukur MM, Obeid MM. First-principle analysis of the structural, mechanical, optical and electronic properties of wollastonite monoclinic polymorph. Computational Condensed Matter 2018;14:20–6.
[48] Weck PF, Kim E, Buck EC. On the mechanical stability of uranyl peroxide hydrates: implications for nuclear fuel degradation. RSC Adv 2015;5(96):79090–7.
[49] Nan-Xi M, et al. Mechanical and thermodynamic properties of the monoclinic and orthorhombic phases of SiC_2N_4 under high pressure from first principles. Chin Phys B 2014;23(12):127101.
[50] Yıldız GD, et al. Computational investigations of mechanic, electronic and lattice dynamic properties of yttrium based compounds. Int J Mod Phys B 2018;32(20):1850214.
[51] Al S, Arikan N, Iyigör A. Investigations of structural, elastic, Electronic and thermodynamic Properties of X_2TiAl alloys: a computational study. Z Naturforsch 2018;73(9):859–67.
[52] Iyigor A. Investigations of structural, elastic, electronic, vibrational and thermodynamic properties of RhMnX (X = Sb and Sn). Mater Res Express 2019;6(11):116110.

[53] Li P, et al. First-principles investigations on structural stability, elastic and electronic properties of Co_7M_6 (M= W, Mo, Nb) μ phases. Mol Simulat 2019;45(9):752–8.
[54] Pugh SF. XCII. Relations between the elastic moduli and the plastic properties of polycrystalline pure metals. Philosophical Magazine and Journal of Science 1954;45(367):823–43.
[55] Liu L, et al. First-principles investigations on structural and elastic properties of orthorhombic TiAl under pressure. Crystals 2017;7(4):111.
[56] Bannikov VV, Shein IR, Ivanovskii AL. Electronic structure, chemical bonding and elastic properties of the first thorium-containing nitride perovskite $TaThN_3$. Phys Status Solidi Rapid Res Lett 2007;1(3):89–91.
[57] Al S, Iyigor A. Structural, electronic, elastic and thermodynamic properties of hydrogen storage magnesium-based ternary hydrides. Chem Phys Lett 2020;743:137184.